

1 **Soil moisture control on sap-flow response to biophysical factors in a desert-shrub**
2 **species, *Artemisia ordosica***

3 **Authors:** Tianshan Zha^{1,3*#}, Duo Qian^{2#}, Xin Jia^{1,3}, Yujie Bai¹, Yun Tian¹, Charles P.-A.
4 Bourque⁴, Wei Feng¹, Bin Wu¹, Heli Peltola⁵

5 ¹. Yanchi Research Station, School of Soil and Water Conservation, Beijing Forestry
6 University, Beijing 100083, China

7 ². Beijing Vocational College of Agriculture, Beijing 102442, China

8 ³. Key Laboratory of State Forestry Administration on Soil and Water Conservation,
9 Beijing Forestry University, Beijing, China

10 ⁴. Faculty of Forestry and Environmental Management, 28 Dineen Drive, PO Box 4400,
11 University of New Brunswick, New Brunswick, E3B5A3, Canada

12 ⁵. Faculty of Science and Forestry, School of Forest Sciences, University of Eastern
13 Finland, Joensuu, FI-80101, Finland

14 #These authors contributed equally to this work.

15

16

17 **Short title: Sap flow in *Artemisia ordosica***

18

19

20 *Correspondence to:* T. Zha (tianshanzha@bjfu.edu.cn),

21

22 **Author Contribution Statement:**

23 Dr.'s Duo Qian and Tianshan Zha contributed equally to the design and implementation of
24 the field experiment, data collection and analysis, and writing the first draft of the manuscript.

25 Dr. Xin Jia gave helpful suggestions concerning the analysis of the field data and contributed
26 to the scientific revision and editing of the manuscript.

27 Prof. Bin Wu contributed to the design of the experiment.

28 Dr.'s Charles P.-A. Bourque and Heli Peltola contributed to the scientific revision and editing
29 of the manuscript.

30 Yujie Bai, Wei Feng, and Yun Tian were involved in the implementation of the experiment
31 and in the revision of the manuscript.

32

33 **Key Message:** This study provides a significant contribution to the understanding of
34 acclimation processes in desert-shrub species to drought-associated stress in dryland
35 ecosystems

36

37 **Conflict of Interest:**

38 This research was financially supported by grants from the National Natural Science
39 Foundation of China (NSFC No. 31670710), the National Basic Research Program of China
40 (Grant No. 2013CB429901), and by the Academy of Finland (Project No. 14921). The
41 project is related to the Finnish-Chinese collaborative research project, EXTREME (2013-
42 2016), between Beijing Forestry University and the University of Eastern Finland, and
43 USCCC. We appreciate Dr. Ben Wang, Sijing Li, Qiang Yang, and others for their help with
44 the fieldwork. **The authors declare that they have no conflict of interest.**

45

46 **Abstract:** Current understanding of acclimation processes in desert-shrub species to drought
47 stress in dryland ecosystems is still incomplete. In this study, we measured sap flow in
48 *Artemisia ordosica* and associated environmental variables throughout the growing seasons
49 of 2013-2014 (May-September period of each year) to better understand the environmental
50 controls on the temporal dynamics of sap flow. We found that the occurrence of drought in
51 the dry year of 2013 during the leaf-expansion and leaf-expanded periods caused sap flow
52 per leaf area (J_s) to decline significantly, resulting in a sizable drop in transpiration. Sap flow
53 per leaf area correlated positively with radiation (R_s), air temperature (T), and vapor pressure
54 deficit (VPD), when volumetric soil water content (VWC) was $> 0.10 \text{ m}^3 \text{ m}^{-3}$. Diurnal J_s was
55 generally ahead of R_s by as much as 6 hours. This lag time, however, decreased with
56 increasing VWC. Relative response of J_s to the environmental variables (i.e., R_s , T , and VPD)
57 varied with VWC, J_s being more biologically-controlled with a low decoupling coefficient
58 and less sensitivity to the environmental variables during periods of dryness. According to
59 this study, soil moisture is shown to control sap-flow (and, therefore, plant-transpiration)
60 response in *Artemisia ordosica* to diurnal variations in biophysical factors. The findings of
61 this study add to the knowledge of acclimation processes in desert-shrub species under
62 drought-associated stress. This knowledge is essential to model desert-shrub-ecosystem
63 functioning under changing climatic conditions.

64 **Keywords:** sap flow; transpiration; cold-desert shrubs; environmental stress; volumetric soil
65 water content

66

67

68 **1. Introduction**

69 Due to the low amount of precipitation and high potential evapotranspiration in desert
70 ecosystems, low soil water availability limits both plant water- and gas-exchange and, as a
71 consequence, limits vegetation productivity (Razzaghi et al., 2011). Therefore, it is important
72 to understand the mechanisms controlling the vegetation-water dynamics under rapidly
73 changing environments (Jacobsen et al., 2007). Grass species are gradually being replaced
74 by shrub and semi-shrub species in arid and semi-arid areas of northwestern China (Yu et al.,
75 2004). This progression is predicted to continue under a changing climate (Asner et al., 2003;
76 Houghton et al., 1999; Pacala et al., 2001). This is mostly because desert shrubs are able to
77 adapt to hot-dry environments by modifying their morphological characteristics, e.g., by (1)
78 minimizing plant-surface area directly exposed to sun and hot air, (2) producing thick
79 epidermal hairs, (3) thickening cuticle, (4) recessing stomata into leaves (Yang and Zhu,
80 2011), and (5) increasing root-to-shoot ratios (Eberbach and Burrows, 2006; Forner et al.,
81 2014). Also, acclimation of physiological characteristics of plants under water stress, by way
82 of e.g., water potential, osmotic regulation, anti-oxidation, and photosynthetic characteristics,
83 assist the plants to maintain a hydrological balance (Huang et al., 2011a). Changes in stomatal
84 conductance and, thus, transpiration may likewise affect plant water use efficiency (Pacala
85 et al., 2001; Vilagrosa et al., 2003).

86 Sap flow can accurately reflect water consumption during plant transpiration. It
87 maintains ecosystem balance through the soil-plant-atmosphere continuum, but is often
88 affected by environment factors (Huang *et al.*, 2010; Zhao et al., 2016). In recent studies, sap
89 flow in *Tamarix elongate* has been observed to be controlled by solar radiation and air
90 temperature, whereas in *Caragana korshinskii* vapor pressure deficit and solar radiation

91 appear to be more important (Jacobsen et al., 2007; Xia et al., 2008). In *Elaeagnus*
92 *angustifolia*, transpiration is observed to peak at noon, i.e., just before stomatal closure at
93 mid-day under water-deficit conditions (Liu et al., 2011). In contrast, transpiration in
94 *Hedysarum scoparium* peaks multiple times during the day (Xia et al., 2007). Sap flow has
95 been observed to decrease rapidly when the volumetric soil water content (VWC) is lower
96 than the water loss through evapotranspiration (Buzkova et al., 2015). In general, desert
97 shrubs can close their stomata to reduce transpiration when exposed to dehydration stress
98 around mid-day. However, differences exist among shrub species with respect to their
99 stomatal response to changes in soil and air moisture deficits (Pacala et al., 2001). For some
100 shrubs, sap-flow response to precipitation varies from an immediate decline after a heavy
101 rainfall to no observable change after a small rainfall event (Asner et al., 2003; Zheng and
102 Wang, 2014). Sap flow has been found to increase with increasing rainfall intensity (Jian et
103 al., 2016). Drought-insensitive shrubs have relatively strong stomatal regulation and,
104 therefore, tend to be insensitive to soil water deficits and rainfall unlike their drought-
105 sensitive counterparts (Du et al., 2011). In general, understanding of the relationship between
106 sap-flow rates in plants and environmental factors is highly inconsistent, varying with plant
107 habitat (Liu et al., 2011).

108 *Artemisia ordosica*, a shallow-rooted desert shrub, is the dominant plant species in the
109 Mu Us Desert of northwestern China. The shrubs have an important role in combating
110 desertification and in stabilizing sand dunes (Li et al., 2010). Increases in air temperature and
111 precipitation variability and associated shorter wet periods and longer intervals of periodic
112 drought are expected to ensue with projected climate change (Lioubimtseva and Henebry,

113 2009). During dry periods of the year, sap flow in *Artemisia ordosica* has been observed to
114 be controlled by VWC at about 30-cm depth in the soil (Li et al., 2014). Sap-flow rate is
115 known to be affected by variation in precipitation patterns. Soil water content, in combination
116 with other environmental factors, may have a significant influence on sap-flow rate (Li et al.,
117 2014; Zheng and Wang, 2014). Thus, understanding the controlling mechanisms of sap flow
118 in desert shrubs as a function of variations in biotic and abiotic factors is greatly needed (Gao
119 et al., 2013; Xu et al., 2007).

120 In this study, we measured stem sap flow in *Artemisia ordosica* and associated
121 environmental variables throughout the growing seasons of 2013-2014 (May-September
122 period of each year) to better understand the environmental controls on the temporal
123 dynamics of sap flow. We believe that our findings will provide further understanding of
124 acclimation processes in desert-shrub species under stress of dehydration.

125

126 **2. Materials and Methods**

127 **2.1 Experimental site**

128 Continuous sap-flow measurements were made at the Yanchi Research Station (37°42'
129 31" N, 107°13' 47" E, 1530 m above mean sea level), Ningxia, northwestern China. The
130 research station is located between the arid and semi-arid climatic zones along the southern
131 edge of the Mu Us Desert. The sandy soil in the upper 10 cm of the soil profile has a bulk
132 density of $1.54 \pm 0.08 \text{ g cm}^{-3}$ (mean \pm standard deviation, n=16). Mean annual precipitation
133 in the region is about 287 mm, of which 62% falls between July and September. Mean annual
134 potential evapotranspiration and air temperature are about 2,024 mm and 8.1°C based on

135 meteorological data (1954-2004) from the Yanchi County weather station. Normally, shrub
136 leaf-expansion, leaf-expanded, and leaf-coloration stages begin in April, June, and
137 September (Chen et al., 2015), respectively.

138

139 **2.2 Measurements of sap flow, leaf area and stomatal conductance**

140 The experimental plot (10 m × 10 m) was located on the western side of Yanchi Research
141 Station in an *Artemisia ordosica*-dominated area. Mean age of the *Artemisia ordosica* was
142 10-years old. Maximum monthly mean leaf area index (LAI) for plant specimens with full
143 leaf expansion was about 0.1 m² m⁻² (Table 1). Over 60% of their roots were
144 distributed in soil depths of 0-60 cm (Zhao et al., 2010; Jia et al., 2016). Five stems of
145 *Artemisia ordosica* were randomly selected within the plot as replicates for sap-flow
146 measurement. Mean height and sapwood area of sampled shrubs were 84 cm and 0.17 cm²,
147 respectively. Sampled stems represented the average size of stems in the plot. A heat balance
148 sensor (Flow32-1K, Dynamax Inc., Houston, USA) was installed at about 15 cm above the
149 ground surface on each of the five stems (Dynamax, 2005). Sap-flow measurements were
150 taken once per minute for each stem. Half-hourly data were recorded by a Campbell CR1000
151 data logger from May 1 to September 30, 2013-2014 (Campbell Scientific, Logan, UT, USA).

152 Leaf area was estimated for each stem every 7-10 days by sampling about 50-70 leaves
153 from five randomly sampled neighbouring shrubs with similar characteristics to the shrubs
154 used for sap-flow measurements. Leaf area was measured immediately at the station
155 laboratory with a portable leaf-area meter (LI-3000, Li-Cor, Lincoln, NE, USA). Leaf area
156 index (LAI) was measured at roughly weekly intervals on a 4×4 grid of 16 quadrats (10 m

157 $\times 10$ m each) within a 100 m \times 100 m plot centered on the flux tower using measurements of
 158 sampled leaves and allometric equations (Jia et al., 2014). Stomatal conductance (g_s) was
 159 measured *in situ* for three to four leaves on each of the sampled shrubs with a LI-6400
 160 portable photosynthesis analyzer (Li-Cor Inc., Lincoln, USA). The g_s measurements were
 161 made every two hours from 7:00 to 19:00 h every ten days from May to September, 2013-
 162 2014.

163 The degree of coupling between the ecosystem surface and the atmospheric boundary
 164 layer was estimated with the decoupling coefficient (Ω). The decoupling coefficient varies
 165 from 0 (i.e., leaf transpiration is mostly controlled by g_s) to 1 (i.e., leaf transpiration is mostly
 166 controlled by radiation). The Ω was calculated as described by Jarvis and McNaughton
 167 (1986):

$$168 \quad \Omega = \frac{\Delta + \gamma}{\Delta + \gamma \left(1 + \frac{g_a}{g_s} \right)}, \quad (1)$$

169 where Δ is the rate of change of saturation vapor pressure vs. temperature (kPa K⁻¹), γ is the
 170 psychrometric constant (kPa K⁻¹), and g_a is the aerodynamic conductance (m s⁻¹; Monteith
 171 and Unsworth, 1990):

$$172 \quad g_a = \left(\frac{u}{u^{*2}} + 6.2u^{*-0.67} \right)^{-1}, \quad (2)$$

173 where u is the wind speed (m s⁻¹) at 6 m above the ground, and u^* is the friction velocity (m
 174 s⁻¹).

175

176 **2.3 Environmental measurements**

177 Shortwave radiation (R_s in W m⁻²; CMP3, Kipp & Zonen, Netherland), air temperature (T in

178 °C), wind speed (u in m s^{-1} , 034B, Met One Instruments Inc., USA), and relative humidity
179 (RH in %; HMP155A, Väisälä, Finland) were measured simultaneously near the sap-flow
180 measurement plot. Half-hourly data were recorded by data logger (CR3000 data logger,
181 Campbell Scientific Inc., USA). VWC at 30-cm depths were monitored with three ECH₂O-
182 5TE soil moisture probes (Decagon Devices, USA). In the analysis, we used half-hourly
183 averages of VWC from the three soil moisture probes. Vapor pressure deficit (VPD in kPa)
184 was calculated from recorded RH and T .

185

186 **2.4 Data analysis**

187 In our analysis, March-May represented spring, June-August summer, and September-
188 November autumn (Chen et al., 2015). Drought days were defined as those days with daily
189 mean VWC $< 0.1 \text{ m}^3 \text{ m}^{-3}$. This is based on a VWC threshold of $0.1 \text{ m}^3 \text{ m}^{-3}$ for J_s (Fig. 1),
190 with J_s increasing as VWC increased, saturating at VWC of $0.1 \text{ m}^3 \text{ m}^{-3}$, and decreasing as
191 VWC continued to increase. The VWC threshold of $0.1 \text{ m}^3 \text{ m}^{-3}$ is equivalent to a relative
192 extractable soil water (REW) of 0.4 for drought conditions (Granier et al., 1999 and 2007;
193 Zeppel et al., 2004 and 2008; Fig. 2d, e). Duration and severity of ‘drought’ were defined
194 based on a VWC threshold and REW of 0.4. REW was calculated as according to equation
195 (3):

$$196 \quad REW = \frac{VWC - VWC_{\min}}{VWC_{\max} - VWC_{\min}} \quad (3)$$

197 where VWC is the specific daily soil water content ($\text{m}^3 \text{ m}^{-3}$), VWC_{\min} and VWC_{\max} are the
198 minimum and maximum VWC during the measurement period in each year, respectively.

199 Sap-flow analysis was conducted using mean data from five sensors. Sap flow per leaf

200 area (J_s) was used in this study, i.e.,

$$201 \quad J_s = \left(\sum_{i=1}^n E_i / A_{li} \right) / n \quad (4)$$

202 where, J_s is the sap flow per leaf area ($\text{kg m}^{-2} \text{h}^{-1}$) or ($\text{kg m}^{-2} \text{d}^{-1}$), E is the measured sap flow
203 of a stem (g h^{-1}), A_l is the leaf area of the sap-flow stem, and “ n ” is the number of stems used
204 ($n = 5$).

205 Transpiration per ground area (T_r) was estimated in this study according to:

$$206 \quad T_r = \left(\sum_{i=1}^n J_s \times LAI \right) / n \quad (5)$$

207 where, T_r is transpiration per ground area (mm d^{-1}), and LAI is the leaf area index (m^2
208 m^{-2}).

209 Linear and non-linear regression were used to analyze abiotic control on sap-flow rate.

210 In order to minimize the effects of different phenophases and rainfall, we used data only from

211 mid-growing season, non-rainy days, and daytime measurements (8:00-20:00), i.e., from

212 June 1 to August 31, with hourly shortwave radiation $> 10 \text{ W m}^{-2}$. Relations between mean

213 sap-flow rates at specific times over a period of 8:00-20:00 and corresponding environmental

214 factors from June 1 to August 31 were derived with linear regression ($p < 0.05$; Fig. 3).

215 Regression slopes were used as indicators of sap-flow sensitivity (degree of response) to the

216 various environmental variables (see e.g., Zha et al., 2013). All statistical analyses were

217 performed with SPSS v. 17.0 for Windows software (SPSS Inc., USA). Significance level

218 was set at 0.05.

219

220 **3. Results**

221 **3.1 Seasonal variations in environmental factors and sap flow**

222 Range of daily means (24-hour mean) for R_s , T , VPD, and VWC during the 2013 growing
223 season (May-September) were 31.1-364.9 W m⁻², 8.8-24.4°C, 0.05-2.3 kPa, and 0.06-0.17
224 m³ m⁻³ (Fig. 2a, b, c, d), respectively, annual means being 224.8 W m⁻², 17.7°C, 1.03 kPa,
225 and 0.08 m³ m⁻³. Corresponding range of daily means for 2014 were 31.0-369.9 W m⁻², 7.1-
226 25.8°C, 0.08-2.5 kPa, and 0.06-0.16 m³ m⁻³ (Fig. 2a, b, c, d), respectively, annual means being
227 234.9 W m⁻², 17.2°C, 1.05 kPa, and 0.09 m³ m⁻³.

228 Total precipitation and number of rainfall events during the 2013 measurement period
229 (257.2 mm and 46 days) were about 5.6% and 9.8% lower than those during 2014 (272.4 mm
230 and 51 days; Fig. 2d), respectively. In 2013, more irregular rainfall events occurred than in
231 2014, with 45.2% of rainfall falling in July and 8.8% in August.

232 Drought mainly occurred in May, June, and August of 2013 and in May and June of
233 2014 (Fig. 2d,e). Both years had dry springs. Over one-month period of summer drought
234 occurred in 2013.

235 Range of daily J_s during the growing season was 0.01-4.36 kg m⁻² d⁻¹ in 2013 and 0.01-
236 2.91 kg m⁻² d⁻¹ in 2014 (Fig. 2f), with annual means of 0.89 kg m⁻² d⁻¹ in 2013 and 1.31 kg m⁻²
237 d⁻¹ in 2014. Mean daily J_s over the growing season of 2013 was 32%, lower than that of
238 2014. Mean daily T_r were 0.05 mm d⁻¹ and 0.07 mm d⁻¹ over the growing season in 2013 and
239 2014 (Fig. 2f), respectively, being 34% lower in 2013 than in 2014. The total T_r over growing
240 season (May 1-September 30) in 2013 and 2014 were 7.3 mm and 10.9 mm, respectively.
241 Seasonal fluctuations in J_s and T_r corresponded with the seasonal pattern in VWC (Fig. 2d,
242 f). Daily mean J_s and T_r decreased or remained nearly constant during dry-soil periods (Fig.
243 2d, f), with the lowest J_s and T_r observed in spring and mid-summer (August) of 2013.

244

245 **3.2 Sap flow response to environmental factors**

246 In summer, J_s increased with increasing VWC (Fig. 2d, f; Fig. 3d). Soil water was shown to
247 modify the response of J_s to environmental factors (Fig. 4). Sap flow increased more rapidly
248 with increases in R_s , T , and VPD under high VWC (i.e., $VWC > 0.1 \text{ m}^3 \text{ m}^{-3}$ in both 2013 and
249 2014) compared with periods with lower VWC (i.e., $VWC < 0.1 \text{ m}^3 \text{ m}^{-3}$ in both 2013 and
250 2014). Sap flow J_s was more sensitive to R_s , T , and VPD under high VWC (Fig. 4), which
251 coincided with a larger regression slope under high VWC conditions.

252 Sensitivity of J_s to environmental variables (in particular, R_s , T , VPD, and VWC) varied
253 depending on the time of a day (Fig. 5). Regression slopes for the relations of J_s - R_s , J_s - T , and
254 J_s -VPD were greater in the morning before 11:00 h, and lower during mid-day and early
255 afternoon (12:00-16:00 h). In contrast, regression slopes of the relation of J_s -VWC were
256 lower in the morning (Fig. 5), increasing thereafter, peaking at ~13:00 h, and subsequently
257 decreasing in late afternoon. Regression slopes of the response of J_s to R_s , T , and VPD in
258 2014 were greater than those in 2013.

259 **3.3 Diurnal changes and hysteresis between sap flow and environmental factors**

260 Diurnal patterns of J_s were similar in both years (Fig. 6), initiating at 7:00 h and increasing
261 thereafter, peaking before noon (12:00 h), and subsequently decreasing thereafter and
262 remaining near zero from 20:00 to 6:00 h. Diurnal changes in g_s were similar to J_s , but
263 peaking about 2 and 1 h earlier than J_s in July and August, respectively (Fig. 6).

264 There were pronounced time lags between J_s and R_s over the two years (Fig. 7), J_s
265 peaking earlier than R_s and, thus, earlier than either VPD or T . These time lags differed
266 seasonally. For example, mean time lag between J_s and R_s was 2 h during July, 5 h during

267 May, and 3 h during June, August, and September of 2013. However, the time lags in 2014
268 were generally shorter than those observed in 2013 (Table 2).

269 Use of normalized variables may remove the influence of J_s and R_s from the data. As a
270 result, clockwise hysteresis loops between J_s and R_s during the growing period were observed
271 (Fig. 7). As R_s increased in the morning, J_s increased until it peaked at ~10:00 h. Sap-flow
272 rate declined with decreasing R_s during the afternoon. Sap flow J_s was higher in the morning
273 than in the afternoon, forming a clockwise hysteresis loop.

274 Diurnal time lag in the relation of J_s - R_s were influenced by VWC (Fig. 8, 9). For
275 example, J_s peaked about 2 h earlier than R_s on days with low VWC (Fig. 8a), 1 h earlier than
276 R_s on days with moderate VWC (Fig. 8b), and at the same time as R_s on days with high VWC
277 (Fig. 8c). Lag hours between J_s and R_s over the growing season were negatively and linearly
278 related to VWC (Fig. 9: Lag (h) = $-133.5 \times \text{VWC} + 12.24$, $R^2 = 0.41$). Effect of VWC on time
279 lags between J_s and R_s was smaller in 2014, with evenly distributed rainfall during the
280 growing season, than in 2013, with a pronounced summer drought (Fig. 9). State variables g_s
281 and Ω showed a significantly increasing trend with increasing VWC in 2013 and 2014,
282 respectively (Fig. 10).

283

284 **4. Discussion and conclusions**

285 **4.1 Sap flow response to environmental factors**

286 Drought tolerance of some plants may be related to lower overall sensitivity of plant
287 physiological attributes to environmental stress and/or stomatal regulation (Huang et al.,
288 2011b; Naithani et al., 2012). In this study, large regression slopes between J_s and the

289 environmental variables (R_s , VPD, and T) in the morning indicated that sap flow was more
290 sensitive to variations in R_s , VPD, and T during the less dry and hot period of the day (Fig.
291 5). Stomatal conductances were the largest in the morning (Fig. 6), which led to increases in
292 water fluxes to the atmosphere as a result of increased R_s , T , and VPD. When R_s peaked
293 during mid-day (13:00-14:00 h), there was often insufficient soil water to meet the
294 atmospheric demand for water, causing g_s to be limited by available soil moisture and making
295 J_s more responsive to VWC at noon, but less responsive to R_s and T . Similarly, *Hedysarum*
296 *mongolicum* in a nearby region positively correlated with VWC at noon (Qian et al., 2015),
297 and the evapotranspiration of a Scots pine stand showed higher sensitivity to surface
298 conductance, temperature, vapor pressure deficit, and radiation in the morning than in the
299 afternoon (Zha et al., 2013).

300 Synergistic interactions among environmental factors influencing sap flow are complex.
301 In general, VWC has an influence on physiological processes of plants in water-limited
302 ecosystems (Lei et al., 2010; She et al., 2013). Our finding regarding lower sensitivity in J_s
303 to environmental factors (R_s , T and VPD) during dry periods was consistent with an earlier
304 study of boreal grasslands (Zha et al., 2010). Also our finding that VWC is the most important
305 factor modifying responses in sap flow in *Artemisia ordosica* to other environmental factors,
306 is in contrast to other shrub species. For example, it has been found that sap flow in *Haloxylon*
307 *ammodendron* in northwest China, where annual precipitation is 37.9 mm and mean annual
308 temperature is 8.2 °C, was mainly controlled by T (Zhang et al., 2003), while sap flow in
309 *Cyclobalanopsis glauca* in south China, where annual precipitation is 1900 mm and mean
310 annual temperature is 19.3 °C, was controlled by R_s and T , when VWC was not limiting

311 (Huang et al., 2009).

312 Precipitation, being the main source of VWC at our site, affected transpiration directly.
313 In this sense, frequent small rainfall events (< 5 mm) were important to the survival and
314 growth of the desert plants (Sala and Lauenroth, 1982; Zhao and Liu, 2010). Variations in J_s
315 were clearly associated with the intermittent supply of water to the soil during rainfall events,
316 as indicated at our site (Fig. 2d, f). Reduced J_s during rainy days can be explained by a
317 reduction in incident R_s and water-induced saturation on the leaf surface, which led to a
318 decrease in leaf turgor and stomatal closure. After each rainfall event, J_s increased quickly
319 when soil water was replenished. Schwinning and Sala (2004) showed previously for similar
320 research sites that VWC contributed the most to the response in plant transpiration to post-
321 rainfall events. We showed in this study that *Artemisia ordosica* responded in a different way
322 to wet and dry conditions. In the mid-growing season, high J_s in July were related to rainfall-
323 fed VWC, which increased the rate of transpiration. However, dry soil conditions combined
324 with high T and R_s , led to a reduction in J_s in August of 2013 (Fig. 2). In some desert shrubs,
325 groundwater may replenish water lost by transpiration by having deep roots (Yin et al., 2014).
326 *Artemisia ordosica* roots are generally distributed in the upper 60 cm of the soil (Zhao et al.,
327 2010; Wang et al., 2016), and as a result the plant usually depends on water directly supplied
328 by precipitation because groundwater levels in drylands can be well below the rooting zone,
329 typically, at depths ≥ 10 m at our site.

330

331 **4.2 Hysteresis between sap flow and environmental factors**

332 Diurnal patterns in J_s corresponded with those of R_s from sunrise until diverging later in the

333 day (Fig. 7), suggesting that R_s was a primary controlling factor of diurnal variation in J_s .
334 According to O'Brien et al. (2004), diurnal variation in R_s could cause change in the diurnal
335 variation in the consumption of water. As an initial energy source, R_s can force T and VPD
336 to increase, causing a phase difference in time lags among the relations J_s - R_s , J_s - T , and J_s -
337 VPD.

338 We found a consistent clockwise hysteresis loop between J_s and R_s over a diurnal cycle
339 (Fig. 7), indicating that R_s lagged J_s , and the response of J_s to R_s varied both diurnally and
340 seasonally. A large g_s in the morning promoted higher rates of transpiration (Fig. 6). In dry
341 and hot conditions, g_s decreased, causing the control of the stomata on J_s to increase relative
342 to changes in environmental factors. Diurnal trends in J_s and g_s occurred together, both
343 peaking earlier than R_s . The g_s peaked 3-4 h earlier than R_s , leading to a reduction in J_s and
344 an increase in R_s and a clockwise hysteresis loop. Contrary to our findings, counterclockwise
345 hysteresis has been observed to occur between transpiration (J_s) and R_s in tropical and
346 temperate forests (Meinzer et al., 1997; O'Brien et al., 2004; Zeppel et al., 2004). A possible
347 reason for this difference may be due to differences in VWC associated with the different
348 regions. According to Zheng and Wang (2014) favorable water conditions after rainfall could
349 render clockwise hysteresis loops between J_s and R_s under dry conditions to counterclockwise
350 loops. In this study, due to a large incidence of small rainfall events, soil water supply by
351 rainfall pulses could not meet the transpiration demand under high mid-day R_s , resulting in
352 clockwise loops even though rainfall had occurred.

353 In semi-arid regions, low VWC restricts plant transpiration more than VPD. Water
354 vapor deficits tend to restrict transpiration in forest species in wet regions to a greater extent.

355 According to Zheng et al. (2014), high water availability in alpine shrubland meadows may
356 contribute to weakened hysteresis between evapotranspiration and the environmental
357 variables. Our results showed that hysteresis between J_s and R_s decreased as VWC increased
358 (Fig. 8, 9). The result that g_s increased with increasing VWC (Fig. 10a), along with the
359 synchronization of J_s and g_s , suggests that J_s is less sensitive to g_s in high VWC and more so
360 to R_s . Temporal patterns in J_s became more consistent with those in R_s as VWC increased,
361 leading to a weakened hysteresis between the two variables. This is further supported by a
362 large decoupling coefficient, when VWC is high (Fig. 10b). The larger the decoupling
363 coefficient is, the greater is the influence of R_s on J_s . The effect of VWC on time lag varied
364 between 2013 and 2014.

365 **4.3. Conclusions**

366 Drought during the leaf-expansion and leaf-expanded periods led to a greater decline in J_s ,
367 causing J_s to be lower in 2013 than in 2014. The relative influence of R_s , T , and VPD on J_s in
368 *Artemisia ordosica* was modified by soil water content, indicating J_s 's lower sensitivity to
369 environmental variables (R_s , T and VPD) during dry periods. Sap flow J_s was constrained by
370 soil water deficiency, causing J_s to peak several hours prior to R_s . Diurnal hysteresis between
371 J_s and R_s varied seasonally, because of the control by stomatal conductance under low VWC
372 and R_s under high VWC. According to this study, soil moisture controlled sap-flow response
373 in *Artemisia ordosica*. This species is capable to tolerate and adapt to soil water deficiencies
374 and drought conditions during the growing season. Altogether, our findings add to our
375 understanding of acclimation in desert-shrub species under stress of dehydration. The
376 knowledge gain can assist in modeling desert-shrub-ecosystem functioning under changing

377 climatic conditions.

378 **Acknowledgments:** This research was financially supported by grants from the National
379 Natural Science Foundation of China (NSFC No. 31670710, 31670708, 31361130340,
380 31270755), the National Basic Research Program of China (Grant No. 2013CB429901), and
381 the Academy of Finland (Project No. 14921). Xin Jia and Wei Feng are also grateful to
382 financial support from the Fundamental Research Funds for the Central Universities (Proj.
383 No. 2015ZCQ-SB-02). This work is related to the Finnish-Chinese collaborative research
384 project EXTREME (2013-2016), between Beijing Forestry University (team led by Prof.
385 Tianshan Zha) and the University of Eastern Finland (team led by Prof. Heli Peltola), and the
386 U.S. China Carbon Consortium (USCCC). We thank Ben Wang, Sijing Li, Qiang Yang, and
387 others for their assistance in the field.

388

389 **References**

- 390 Asner, G. P., Archer, S., Hughes, R. F., Ansley, R. J., and Wessman, C. A.: Net changes in regional woody
391 vegetation cover and carbon storage in Texas Drylands, 1937–1999, *Global Change Biol.*, 9, 316-
392 335, 2003.
- 393 Buzkova, R., Acosta, M., Darenova, E., Pokorny, R., and Pavelka, M.: Environmental factors influencing
394 the relationship between stem CO₂ efflux and sap flow, *Trees-Struct. Funct.*, 29, 333-343, 2015.
- 395 Chen, Z., Zha, T. S., Jia, X., Wu, Y., Wu, B., Zhang, Y., Guo, J., Qin, S., Chen, G., Peltola, H.: Leaf
396 nitrogen is closely coupled to phenophases in a desert shrub ecosystem in China, *J. Arid Environ.*,
397 120, 33-41, 2015. Du, S., Wang, Y. L., Kume, T., Zhang, J. G., Otsuki, K., Yamanaka, N., and Liu,
398 G. B.: Sapflow characteristics and climatic responses in three forest species in the semiarid Loess

399 Plateau region of China, *Agr. Forest Meteorol.*, 151, 1-10, 2011.

400 Dynamax: Dynagage® Installation and Operation Manual, Dynamax, Houston, TX, 2005.

401 Eberbach, P. L. and Burrows, G. E.: The transpiration response by four topographically distributed
402 Eucalyptus species, to rainfall occurring during drought in south eastern Australia, *Physiol. Plant.*,
403 127, 483-493, 2006.

404 Forner, A., Aranda, I., Granier, A., and Valladares, F.: Differential impact of the most extreme drought
405 event over the last half century on growth and sap flow in two coexisting Mediterranean trees, *Plant*
406 *Ecol.*, 215, 703-719, 2014.

407 Gao, Q., Yu, M., and Zhou, C.: Detecting the Differences in Responses of Stomatal Conductance to
408 Moisture Stresses between Deciduous Shrubs and Artemisia Subshrubs, *Plos One*, 8, e84200, 2013.

409 Granier, A., Bréda, N., Biron, P., and Villette, S.: A lumped water balance model to evaluate duration and
410 intensity of drought constraints in forest stands. *Ecol. Model.*, 116, 269–283, 1999.

411 Granier, A., Reichstein M., Bréda N., Janssens I. A., Falge E., Ciais P., Grünwald T., Aubinet M.,
412 Berbigier P., Bernhofer C., Buchmann N., Facini O., Grassi G., Heinesch B., Ilvesniemi H., Kerone
413 P., Knohl A., Köstner B., Lagergren F., Lindroth A., Longdoz B., Loustau D., Mateus J., Montagnani
414 L., Nys C., Moors E., Papale D., Peiffer M., Pilegaard K., Pita G., Pumpanen J., Rambal S., Rebmann
415 C., Rodrigues A., Seufert G., Tenhunen J., Vesala T., and Wang Q.: Evidence for soil water control
416 on carbon and water dynamics in European forests during the extremely dry year: 2003. *Agr. Forest*
417 *Meteorol.*, 143, 123-145, 2007.

418 Houghton, R. A., Hackler, J. L., and Lawrence, K. T.: The U.S. Carbon Budget: Contributions from Land-
419 Use Change, *Science*, 285, 574-578, 1999.

420 Huang, L., Zhang, Z. S., and Li, X. R.: Sap flow of *Artemisia ordosica* and the influence of environmental

421 factors in a revegetated desert area: Tengger Desert, China. *Hydrol. Process.*, 24, 1248–1253, 2010.

422 Huang, H., Gang, W., and NianLai, C.: Advanced studies on adaptation of desert shrubs to environmental
423 stress, *Sci. Cold Arid Regions*, 3, 0455–0462, 2011a.

424 Huang, Y., Li, X., Zhang, Z., He, C., Zhao, P., You, Y., and Mo, L.: Seasonal changes in *Cyclobalanopsis*
425 *glauca* transpiration and canopy stomatal conductance and their dependence on subterranean water
426 and climatic factors in rocky karst terrain, *J. Hydrol.*, 402, 135-143, 2011b.

427 Huang, Y., Zhao, P., Zhang, Z., Li, X., He, C., and Zhang, R.: Transpiration of *Cyclobalanopsis glauca*
428 (syn. *Quercus glauca*) stand measured by sap-flow method in a karst rocky terrain during dry season,
429 *Ecol. Res.*, 24, 791-801, 2009.

430 Jacobsen, A. L., Agenbag, L., Esler, K. J., Pratt, R. B., Ewers, F. W., and Davis, S. D.: Xylem density,
431 biomechanics and anatomical traits correlate with water stress in 17 evergreen shrub species of the
432 Mediterranean-type climate region of South Africa, *J. Ecol.*, 95, 171-183, 2007.

433 Jarvis, P. G. and McNaughton, K. G.: Stomatal Control of Transpiration: Scaling Up from Leaf to Region.
434 In: *Advances in Ecological Research*, MacFadyen, A. and Ford, E. D. (Eds.), Academic Press, 1986.

435 Jia, X., Zha, T.S., Wu, B., Zhang, Y., Gong, J., Qin, S., Chen, G., Kellomki, S. & Peltola, H.: Biophysical
436 controls on net ecosystem CO₂ exchange over a semiarid shrubland in northwest China.
437 *Biogeosciences*, 11, 4679-4693, 2014.

438 Jia, X., Zha, T. S, Gong, J., Wang, B., Zhang Y., Wu B., Qin S., and Peltola H.: Carbon and water exchange
439 over a temperate semi-arid shrubland during three years of contrasting precipitation and soil
440 moisture patterns. *Agr. Forest Meteorol.*, 228, 120-129, 2016.

441 Jian, S. Q., Wu, Z. N., Hu, C. H., and Zhang, X. L.: Sap flow in response to rainfall pulses for two shrub
442 species in the semiarid Chinese Loess Plateau, *J. Hydrol. Hydromech.*, 64, 121-132, 2016.

443 Lei, H., Zhi-Shan, Z., and Xin-Rong, L.: Sap flow of *Artemisia ordosica* and the influence of
444 environmental factors in a revegetated desert area: Tengger Desert, China, *Hydrol. Process.*, 24,
445 1248-1253, 2010.

446 Li, S., Werger, M. A., Zuidema, P., Yu, F., and Dong, M.: Seedlings of the semi-shrub *Artemisia ordosica*
447 are resistant to moderate wind denudation and sand burial in Mu Us sandland, China, *Trees*, 24, 515-
448 521, 2010.

449 Li, S., Zha, T., Qin, S., Qian, D., and Jia, X.: Temporal patterns and environmental controls of sap flow in
450 *Artemisia ordosica*, *Chinese J. Ecol.*, 33, 1-7, 2014.

451 Lioubimtseva, E. and Henebry, G. M.: Climate and environmental change in arid Central Asia: Impacts,
452 vulnerability, and adaptations, *J. Arid Environ.*, 73, 963-977, 2009.

453 Liu, B., Zhao, W., and Jin, B.: The response of sap flow in desert shrubs to environmental variables in an
454 arid region of China, *Ecohydrology*, 4, 448-457, 2011.

455 Meinzer, F. C., Andrade, J. L., Goldstein, G., Holbrook, N. M., Cavelier, J., and Jackson, P.: Control of
456 transpiration from the upper canopy of a tropical forest: the role of stomatal, boundary layer and
457 hydraulic architecture components, *Plant Cell Environ.*, 20, 1242-1252, 1997.

458 Monteith, J. L. and Unsworth, M. H.: *Principles of Environmental Physics*. Butterworth-Heinemann:
459 Oxford, 1990.

460 Naithani, K. J., Ewers, B. E., and Pendall, E.: Sap flux-scaled transpiration and stomatal conductance
461 response to soil and atmospheric drought in a semi-arid sagebrush ecosystem, *J. Hydrol.*, 464, 176-
462 185, 2012.

463 O'Brien, J. J., Oberbauer, S. F., and Clark, D. B.: Whole tree xylem sap flow responses to multiple
464 environmental variables in a wet tropical forest, *Plant Cell Environ.*, 27, 551-567, 2004.

465 Pacala, S. W., Hurtt, G. C., Baker, D., Peylin, P., Houghton, R. A., Birdsey, R. A., Heath, L., Sundquist,
466 E. T., Stallard, R. F., Ciais, P., Moorcroft, P., Caspersen, J. P., Shevliakova, E., Moore, B., Kohlmaier,
467 G., Holland, E., Gloor, M., Harmon, M. E., Fan, S.-M., Sarmiento, J. L., Goodale, C. L., Schimel, D.,
468 and Field, C. B.: Consistent Land- and Atmosphere-Based U.S. Carbon Sink Estimates, *Science*, 292,
469 2316-2320, 2001.

470 Qian, D., Zha, T. S., Jia, X., Wu, B., Zhang, Y., Bourque C. P. A., Qin, S., and Peltola, H.: Adaptive,
471 water-conserving strategies in *Hedysarum mongolicum* endemic to a desert shrubland ecosystem,
472 *Environ. Earth. Sci.*, 74, 6039–6046, 2015.

473 Razzaghi, F., Ahmadi, S. H., Adolf, V. I., Jensen, C. R., Jacobsen, S. E., and Andersen, M. N.: Water
474 Relations and Transpiration of Quinoa (*Chenopodium quinoa* Willd.) Under Salinity and Soil Drying,
475 *J. Agron. Crop Sci.*, 197, 348-360, 2011.

476 Sala, O. E., and Lauenroth, W. K.: Small rainfall events: an ecological role in semi-arid regions, *Oecologia*,
477 53 (3), 301-304, 1982.

478 Schwinning, S. and Sala, O. E.: Hierarchy of responses to resource pulses in arid and semi-arid ecosystems,
479 *Oecologia*, 141, 211-220, 2004.

480 She, D., Xia, Y., Shao, M., Peng, S., and Yu, S.: Transpiration and canopy conductance of *Caragana*
481 *korshinskii* trees in response to soil moisture in sand land of China, *Agroforest. syst.*, 87, 667-678,
482 2013.

483 Vilagrosa, A., Bellot, J., Vallejo, V. R., and Gil- Pelegrín, E.: Cavitation, stomatal conductance, and leaf
484 dieback in seedlings of two co- occurring Mediterranean shrubs during an intense drought, *J. Exp.*
485 *Bot.*, 54, 2015-2024, 2003.

486 Wang, B., Zha, T. S., Jia, X., Gong, J.N., Wu, B., Bourque, C. P. A., Zhang, Y., Qin, S., Chen, G., Peltola,

487 H.: Microtopographic variation in soil respiration and its controlling factors vary with plant
488 phenophases in a desert–shrub ecosystem. *Biogeosciences*, 12, 5705-5714, 2015.

489 Xia, G., Kang, S., Du, T., Yang, X., and Zhang, J.: Transpiration of *Hedysarum scoparium* in arid desert
490 region of Shiyang River basin, Gansu Province, *Chinese J. Appl. Ecol.*, 18, 1194-1202, 2007.

491 Xia, G., Kang, S., Li, F., Zhang, J., and Zhou, Q.: Diurnal and seasonal variations of sap flow of *Caragana*
492 *korshinskii* in the arid desert region of north-west China, *Hydrol. Process.*, 22, 1197-1205, 2008.

493 Xu, D. H., Li, J. H., Fang, X. W., and Wang, G.: Changes in soil water content in the rhizosphere of
494 *Artemisia ordosica*: Evidence for hydraulic lift, *J. Arid Environ.*, 69, 545-553, 2007.

495 Yang, Y. and Zhu, Y.: *Plant Ecology (Second Edition)*, Higher Education Press, Beijing, 2011.

496 Yin, L., Zhou, Y., Huang, J., Wenninger, J., Hou, G., Zhang, E., Wang, X., Dong, J., Zhang, J., and
497 Uhlenbrook, S.: Dynamics of willow tree (*Salix matsudana*) water use and its response to
498 environmental factors in the semi-arid Hailiutu River catchment, Northwest China, *Environ. earth*
499 *sci.*, 71, 4997-5006, 2014.

500 Yu, M., , Ellis, J. E., and Epstein, H. E.: Regional analysis of climate, primary production, and livestock
501 density in Inner Mongolia. *J. Environ. Qual.*, 33(5), 1675-1681, 2004.

502 Zeppel, M. J. B., Murray, B. R., Barton, C., and Eamus, D.: Seasonal responses of xylem sap velocity to
503 VPD and solar radiation during drought in a stand of native trees in temperate Australia, *Funct. Plant*
504 *Biol.*, 31, 461-470, 2004.

505 Zeppel, M. J. B., Macinnis-Ng, C. M. O., Yunusa, I. A. M., Whitley, R. J., and Eamus, D. Long term
506 trends of stand transpiration in a remnant forest during wet and dry years, *J. Hydrol.*, 349, 200-213,
507 2008.

508 Zha, T. S., Barr, A. G., Kamp, G. V. D., Black, T.A., McCaughey, J. H., and Flanagan, L.B.: Interannual

509 variation of evapotranspiration from forest and grassland ecosystems in western Canada in relation
510 to drought, *Agr. Forest Meteorol.*, 150, 1476-1484, 2010.

511 Zha, T. S., Li, C., Kellomäki, S., Peltola, H., Wang, K.-Y., and Zhang, Y.: Controls of Evapotranspiration
512 and CO₂ Fluxes from Scots Pine by Surface Conductance and Abiotic Factors, *Plos One*, 8, e69027,
513 2013.

514 Zhang, X., Gong, J., Zhou, M., and Si, J.: A study on the stem sap flow of *Populus euphratica* and *Tamaris*
515 spp. By heat pulse technique, *J. Glaciol. Geocryol.*, 25, 584-590, 2003.

516 Zhao, W. and Liu, B.: The response of sap flow in shrubs to rainfall pulses in the desert region of China,
517 *Agr. Forest Meteorol.*, 150, 1297-1306, 2010.

518 Zhao, Y., Yuan, W., Sun, B., Yang, Y., Li, J., Li, J., Cao, B., and Zhong, H.: Root Distribution of Three
519 Desert Shrubs and Soil Moisture in Mu Us Sand Land. *Res. Soil Water Conserv.*, 17, 129-133, 2010.

520 Zhao, W., Liu, B., Chang, X., Yang, Q., Yang, Y., Liu Z., Cleverly, J., and Eamus, D.: Evapotranspiration
521 partitioning, stomatal conductance, and components of the water balance: A special case of a desert
522 ecosystem in China. *J. Hydrol.*, 538, 374-386, 2016.

523 Zheng, C. and Wang, Q.: Water-use response to climate factors at whole tree and branch scale for a
524 dominant desert species in central Asia: *Haloxylon ammodendron*, *Ecohydrology*, 7, 56-63, 2014.

525 Zheng, H., Wang, Q., Zhu, X., Li, Y., and Yu, G.: Hysteresis Responses of Evapotranspiration to
526 Meteorological Factors at a Diel Timescale: Patterns and Causes, *Plos One*, 9, e98857, 2014.

527

528

529

530 **Table 1** Seasonal changes in monthly transpiration (T_r), leaf area index (LAI), and stomatal
 531 conductance (g_s) of *Artemisia ordosica* from 2013 to 2014.
 532

	T_r (mm mon ⁻¹)		LAI (m ² m ⁻²)		g_s (mol m ⁻² s ⁻¹)	
	2013	2014	2013	2014	2013	2014
May	0.57	1.59	0.02	0.04	0.07	0.18
June	1.03	2.28	0.05	0.06	0.08	0.13
July	3.36	3.46	0.10	0.06	0.09	0.14
August	1.04	2.45	0.08	0.06	0.10	0.08
September	1.23	1.13	0.05	0.04	0.15	0.05

533
 534

535 **Table 2** Mean monthly diurnal cycles of sap-flow rate (J_s) response to shortwave radiation
 536 (R_s), air temperature (T), and vapor pressure deficit (VPD), including time lags (h) in J_s as a
 537 function of R_s , T , and VPD.

538

Pattern	May		June		July		August		September	
	2013	2014	2013	2014	2013	2014	2013	2014	2013	2014
J_s - R_s	5	2	3	0	2	1	3	1	3	2
J_s - T	8	6	7	4	4	4	6	5	6	6
J_s -VPD	8	5	7	4	6	4	6	5	6	5

539

540

541

542 **Figure captions:**

543 **Fig. 1** Sap-flow rate per leaf area (J_s) as a function of soil water content (VWC) at 30 cm
544 depth in non-rainy, daytime hours during the mid-growing period from June 1-August 31
545 over 2013-2014. Data points are binned values from pooled data over two years at a VWC
546 increment of $0.003 \text{ m}^3 \text{ m}^{-3}$. Dotted line represents the VWC threshold for J_s .

547 **Fig. 2** Seasonal changes in daily (24-hour) mean shortwave radiation (R_s ; a), air temperature
548 (T ; b), vapor pressure deficit (VPD; c), volumetric soil water content (VWC; d), relative
549 extractable water (REW; e), daily total precipitation (PPT; d), and daily sap-flow per leaf
550 area (J_s ; f), and daily transpiration (T_r , mm d^{-1} ; f) from May to September for both 2013 and
551 2014. Horizontal dash lines (d, e) represent VWC and REW threshold of $0.1 \text{ m}^3 \text{ m}^{-3}$ and 0.4 ,
552 respectively. Shaded bands indicate periods of drought.

553 **Fig. 3** Relationships between sap-flow rate per leaf area (J_s) and environmental factors
554 [shortwave radiation (R_s), air temperature (T), vapor pressure deficit (VPD), and soil water
555 content at 30-cm depth (VWC)] in non-rainy days between 8:00-20:00 h during the mid-
556 growing season of June 1-August 31 for 2013 and 2014. Data points are binned values from
557 pooled data over two years at increments of 40 W m^{-2} , $1.2 \text{ }^\circ\text{C}$, 0.3 kPa , and $0.005 \text{ m}^3 \text{ m}^{-3}$ for
558 R_s , T , VPD and VWC, respectively.

559 **Fig. 4** Sap-flow rate per leaf area (J_s) in non-rainy, daytime hours during the mid-growing
560 season of June 1-August 31 for both 2013 and 2014 as a function of shortwave radiation (R_s),
561 air temperature (T), vapor pressure deficit (VPD) under high volumetric soil water content
562 ($\text{VWC} > 0.10 \text{ m}^3 \text{ m}^{-3}$ both in 2013 and 2014) and low VWC ($< 0.10 \text{ m}^3 \text{ m}^{-3}$, 2013 and 2014).
563 J_s is given as binned averages according to R_s , T , and VPD, based on increments of 100 W

564 m^{-2} , 1°C , and 0.2 kPa , respectively. Bars indicate standard error.

565 **Fig. 5** Regression slopes of linear fits between sap-flow rate per leaf area (J_s) in non-rainy
566 days and shortwave radiation (R_s), vapor pressure deficit (VPD), air temperature (T), and
567 volumetric soil water content (VWC) between 8:00-20:00 h during the mid-growing season
568 of June 1-August 31 for 2013 and 2014.

569 **Fig. 6** Mean monthly diurnal changes in sap-flow rate per leaf area (J_s) and stomatal
570 conductance (g_s) in *Artemisia ordosica* during the growing season (May-September) for both
571 2013 and 2014. Each point is given as the mean at specific times during each month.

572 **Fig. 7** Seasonal variation in hysteresis loops between sap-flow rate per leaf area (J_s) and
573 shortwave radiation (R_s) using normalized plots for both 2013 and 2014. The y-axis
574 represents the proportion of maximum J_s (dimensionless), and the x-axis represents the
575 proportion of maximum R_s (dimensionless). The curved arrows indicate the clockwise
576 direction of response during the day.

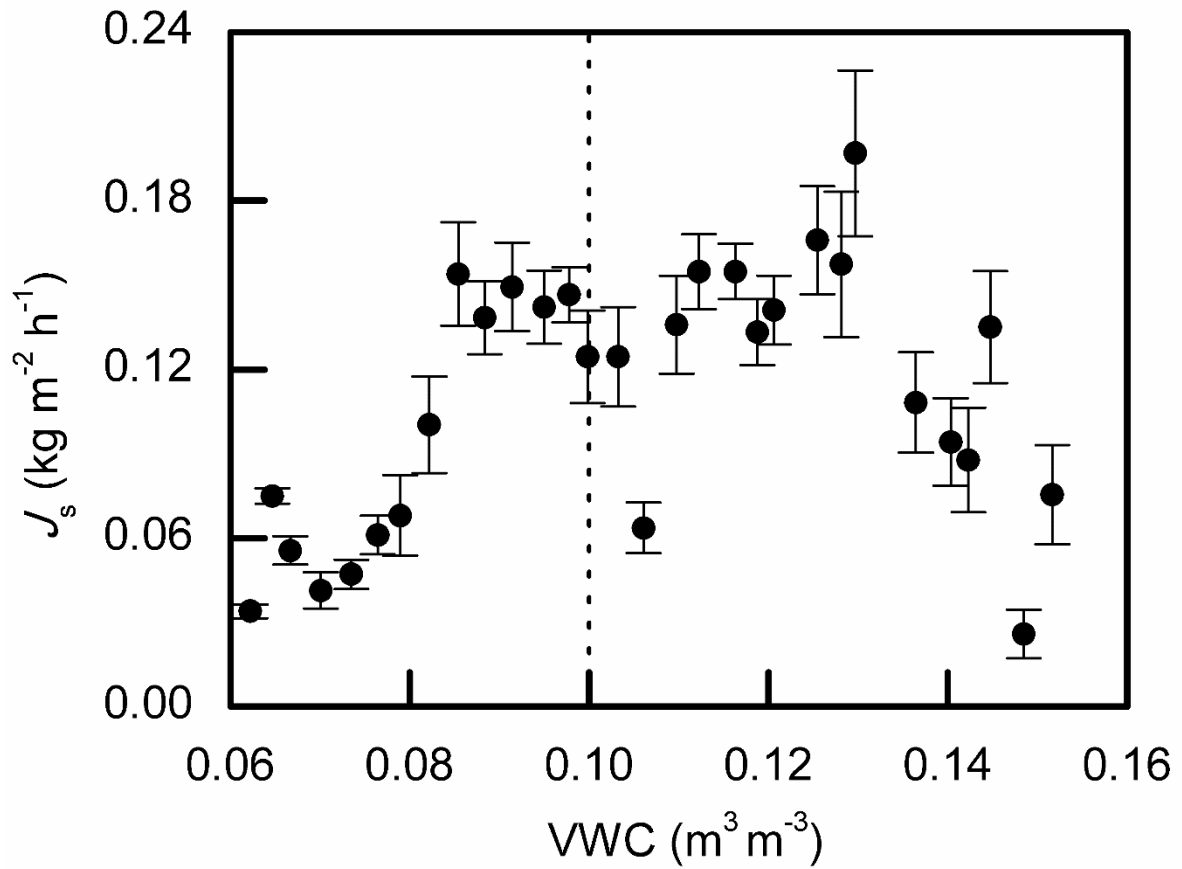
577 **Fig. 8** Sap-flow rate per leaf area (J_s) and shortwave radiation (R_s) over consecutive three
578 days in 2013, i.e., (a) under low volumetric soil water content (VWC) and high vapor pressure
579 deficit (VPD; DOY 153-155, $\text{VWC}=0.064 \text{ m}^3 \text{ m}^{-3}$, $\text{REW}=0.025$, $\text{VPD}=2.11 \text{ kPa}$), (b)
580 moderate VWC and VPD (DOY 212-214, $\text{VWC}=0.092 \text{ m}^3 \text{ m}^{-3}$, $\text{REW}=0.292$, $\text{VPD}=1.72$
581 kPa), and (c) high VWC and low VPD (DOY 192-194, $\text{VWC}=0.152 \text{ m}^3 \text{ m}^{-3}$, $\text{REW}=0.865$,
582 $\text{VPD}= 0.46 \text{ kPa}$). REW is the relative extractable soil water. VWC, REW, and VPD are the
583 mean value of the three days.

584 **Fig. 9** Time lag between sap-flow rate per leaf area (J_s) and short wave radiation (R_s) in
585 relation to volumetric soil water content (VWC). Hourly data in non-rainy days during the

586 mid-growing season of June 1-August 31 for 2013 and 2014. The lag hours were calculated
587 by a cross-correlation analysis using a three-day moving window with a one-day time step.
588 Rainy days were excluded. The solid line is based on exponential regression ($p < 0.05$).

589 **Fig. 10** Relationship between volumetric soil water content (VWC) and (a) stomatal
590 conductance (g_s) in *Artemisia ordosica*, and (b) decoupling coefficient (Ω) for 2013 and 2014.
591 Hourly values are given as binned averages based on a VWC-increment of $0.005 \text{ m}^3 \text{ m}^{-3}$.
592 Bars indicate standard error. Only regressions with p -values < 0.05 are shown.

593

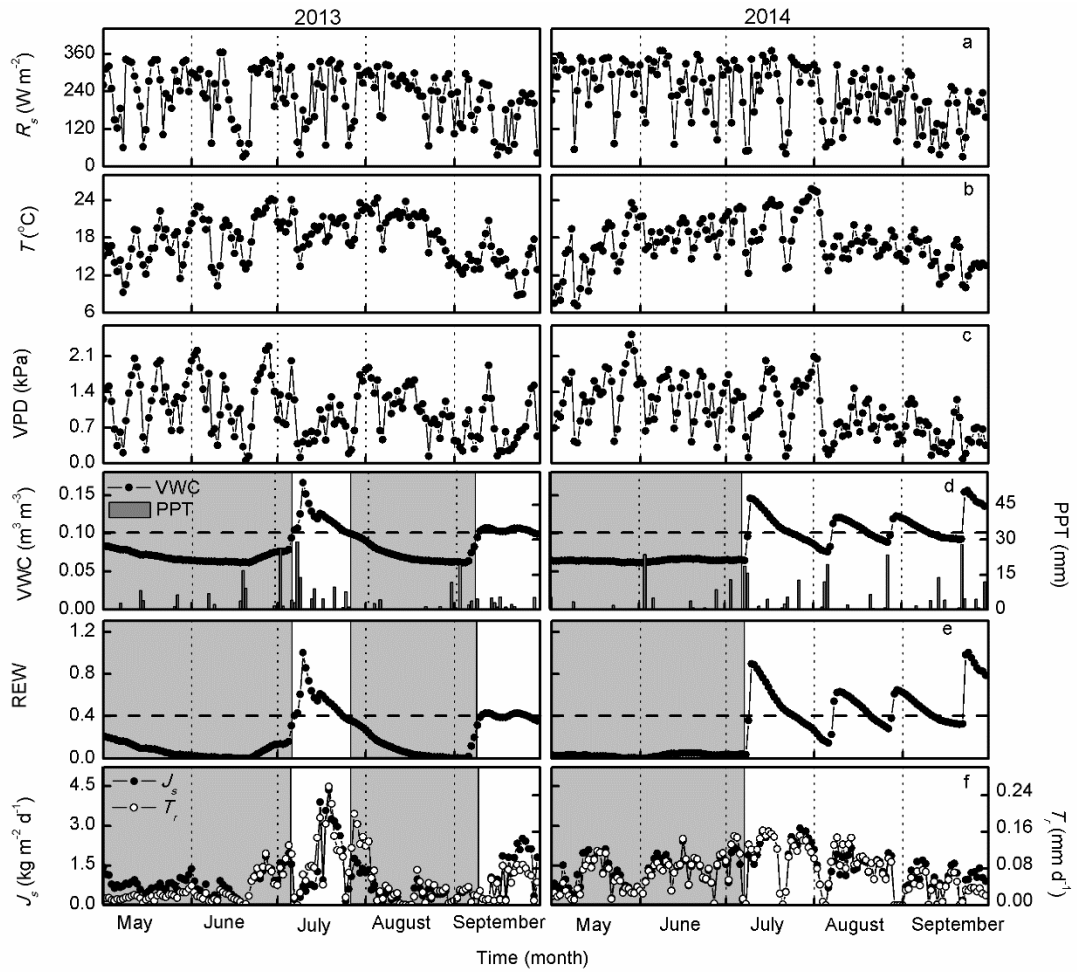


595

596 **Fig. 1** Sap-flow rate per leaf area (J_s) as a function of soil water content (VWC) at 30 cm
 597 depth in non-rainy, daytime hours during the mid-growing period from June 1-August 31
 598 over 2013-2014. Data points are binned values from pooled data over two years at a VWC
 599 increment of $0.003 \text{ m}^3 \text{m}^{-3}$. Dotted line represents the VWC threshold for J_s .

600

601

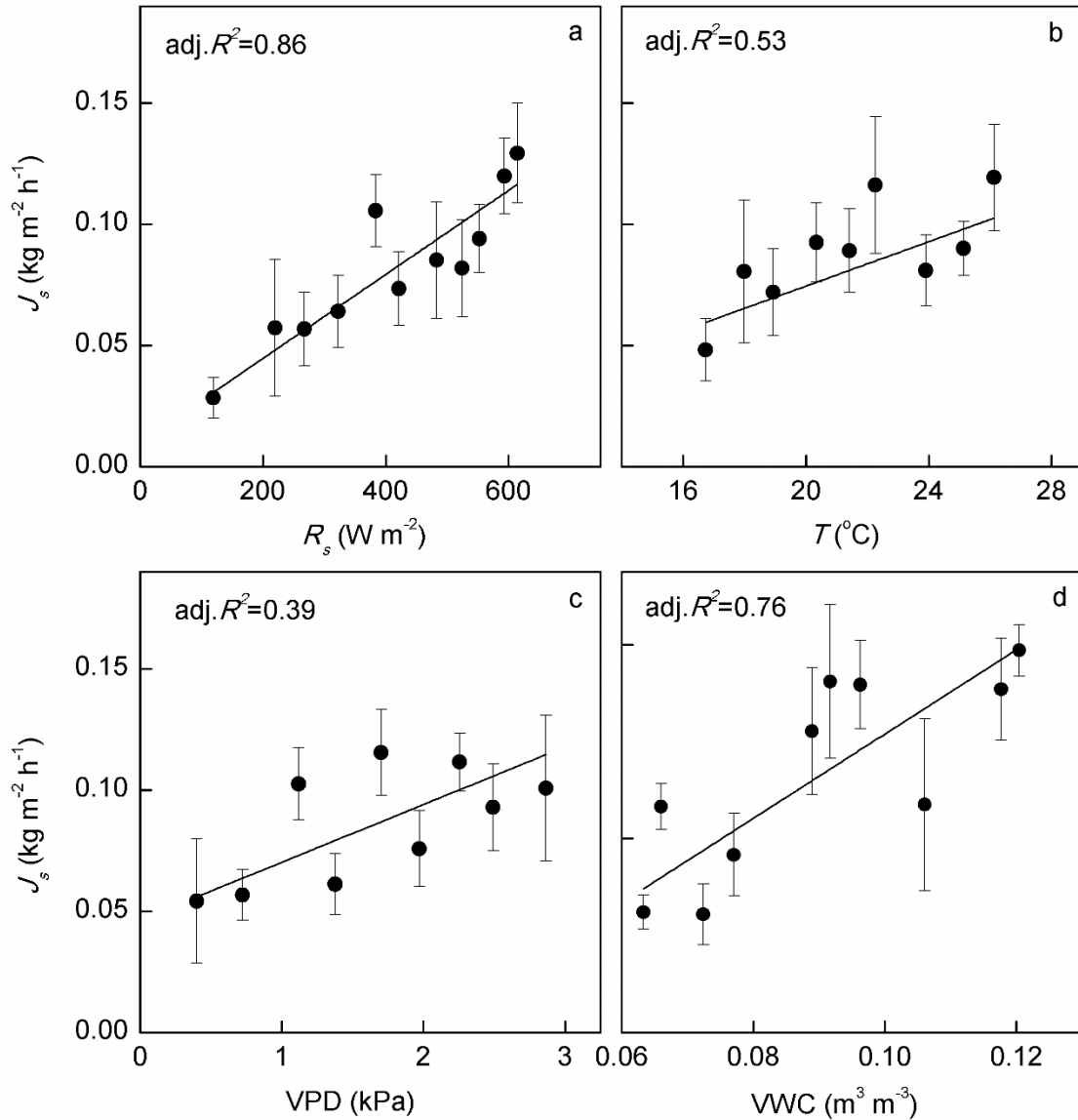


603

604

605 **Fig. 2** Seasonal changes in daily (24-hour) mean shortwave radiation (R_s ; a), air temperature
 606 (T ; b), vapor pressure deficit (VPD; c), volumetric soil water content (VWC; d), relative
 607 extractable water (REW; e), daily total precipitation (PPT; d), and daily sap-flow per leaf
 608 area (J_s ; f), and daily transpiration (T_r , mm d^{-1} ; f) from May to September for both 2013 and
 609 2014. Horizontal dash lines (d, e) represent VWC and REW threshold of $0.1 \text{ m}^3 \text{ m}^{-3}$ and 0.4 ,
 610 respectively. Shaded bands indicate periods of drought.

611



612

613

614 **Fig. 3** Relationships between sap-flow rate per leaf area (J_s) and environmental factors

615 [shortwave radiation (R_s), air temperature (T), vapor pressure deficit (VPD), and soil water

616 content at 30-cm depth (VWC)] in non-rainy days between 8:00-20:00 h during the mid-

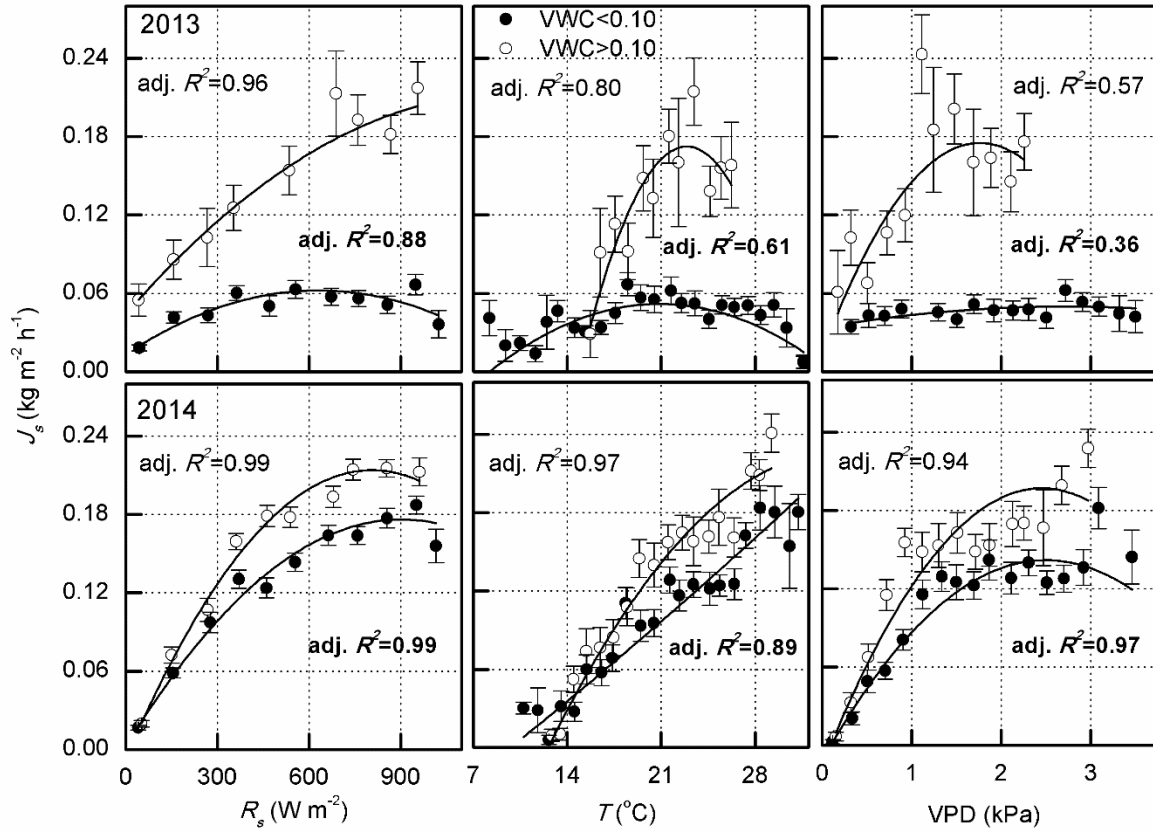
617 growing season of June 1-August 31 for 2013 and 2014. Data points are binned values from

618 pooled data over two years at increments of 40 W m^{-2} , $1.2 \text{ }^{\circ}\text{C}$, 0.3 kPa , and $0.005 \text{ m}^3 \text{ m}^{-3}$ for

619 R_s , T , VPD and VWC, respectively.

620

621



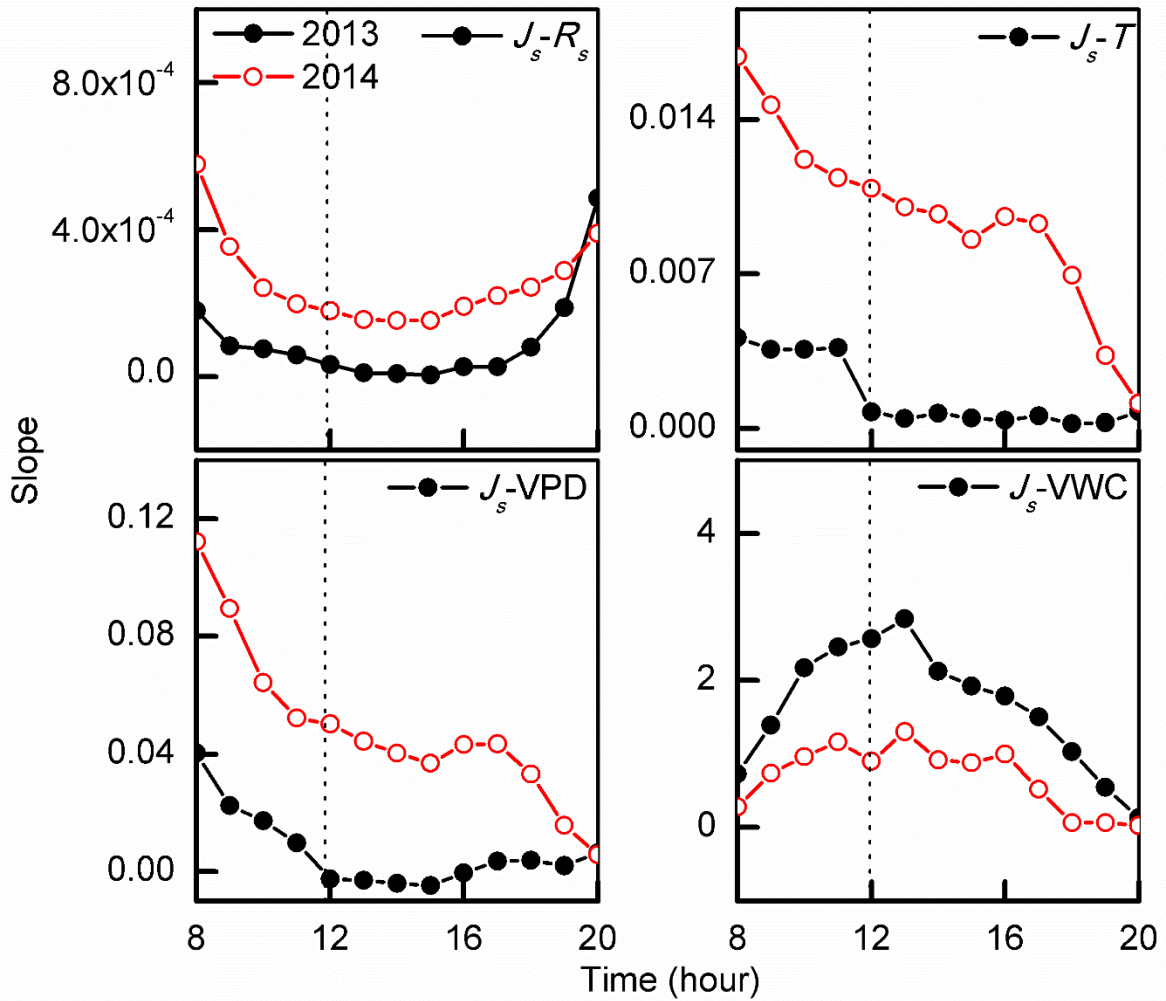
622

623

624 **Fig. 4** Sap-flow rate per leaf area (J_s) in non-rainy, daytime hours during the mid-growing
 625 season of June 1-August 31 for both 2013 and 2014 as a function of shortwave radiation (R_s),
 626 air temperature (T), vapor pressure deficit (VPD) under high volumetric soil water content
 627 ($\text{VWC} > 0.10 \text{ m}^3 \text{ m}^{-3}$ both in 2013 and 2014) and low VWC ($< 0.10 \text{ m}^3 \text{ m}^{-3}$, 2013 and 2014).

628 J_s is given as binned averages according to R_s , T , and VPD, based on increments of 100 W
 629 m^{-2} , 1°C , and 0.2 kPa, respectively. Bars indicate standard error.

630



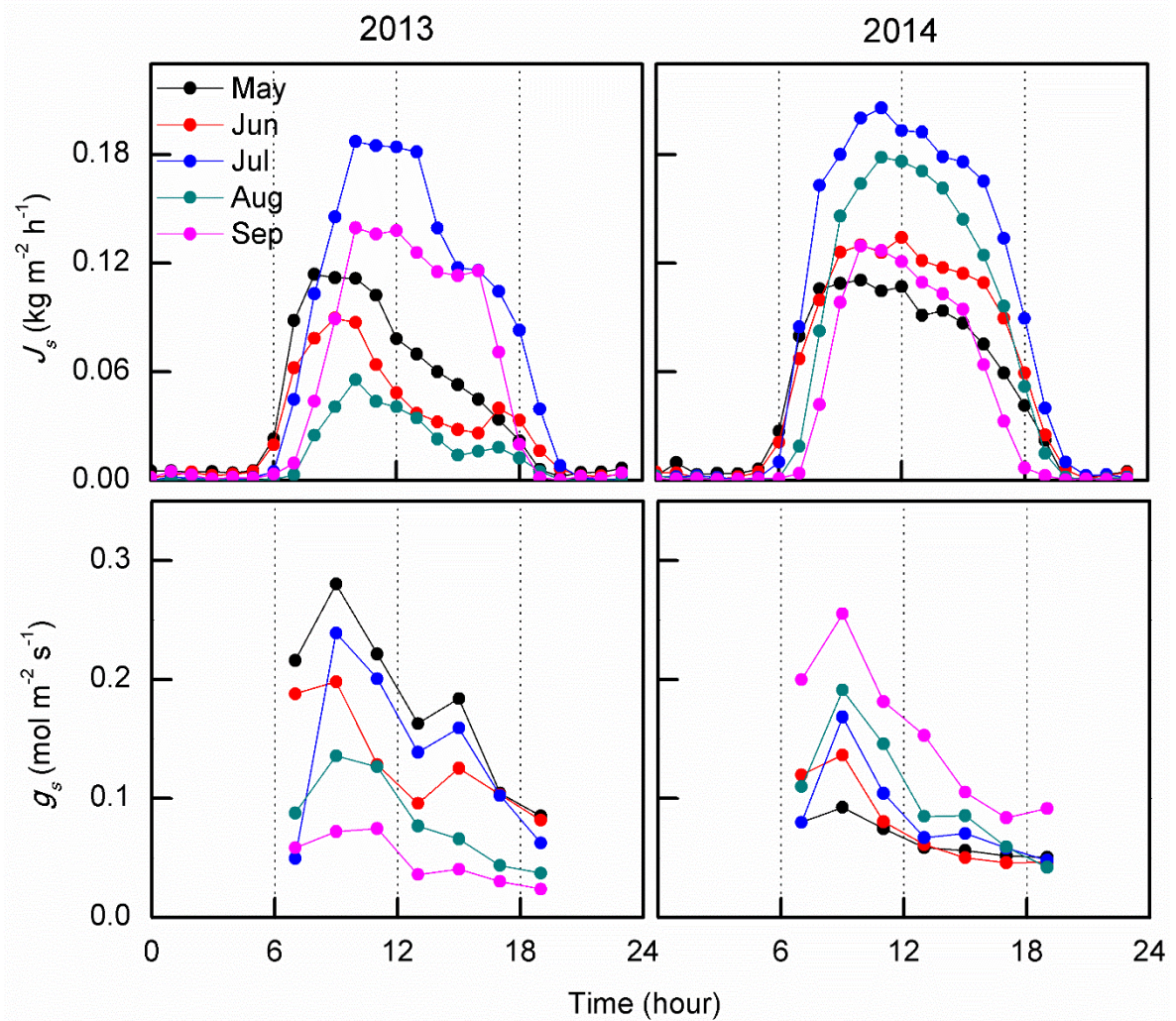
632

633 **Fig. 5** Regression slopes of linear fits between sap-flow rate per leaf area (J_s) in non-rainy634 days and shortwave radiation (R_s), vapor pressure deficit (VPD), air temperature (T), and

635 volumetric soil water content (VWC) between 8:00-20:00 h during the mid-growing season

636 of June 1-August 31 for 2013 and 2014.

637



639

640

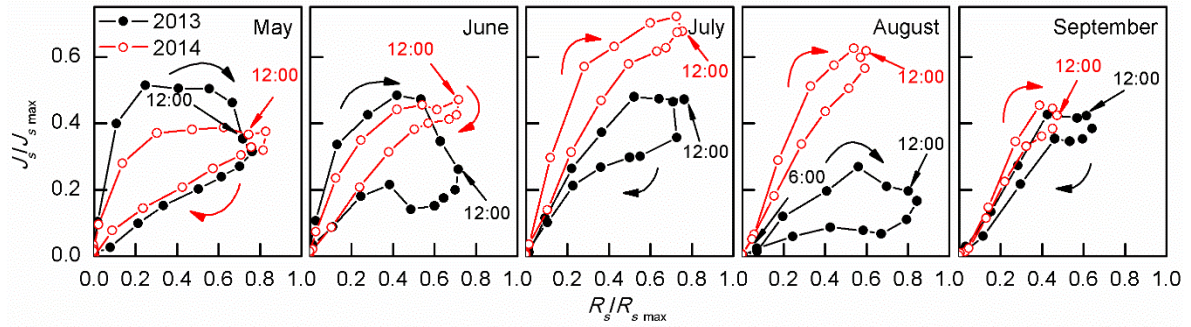
641 **Fig. 6** Mean monthly diurnal changes in sap-flow rate per leaf area (J_s) and stomatal642 conductance (g_s) in *Artemisia ordosica* during the growing season (May-September) for both

643 2013 and 2014. Each point is given as the mean at specific times during each month.

644

645

646



647

648

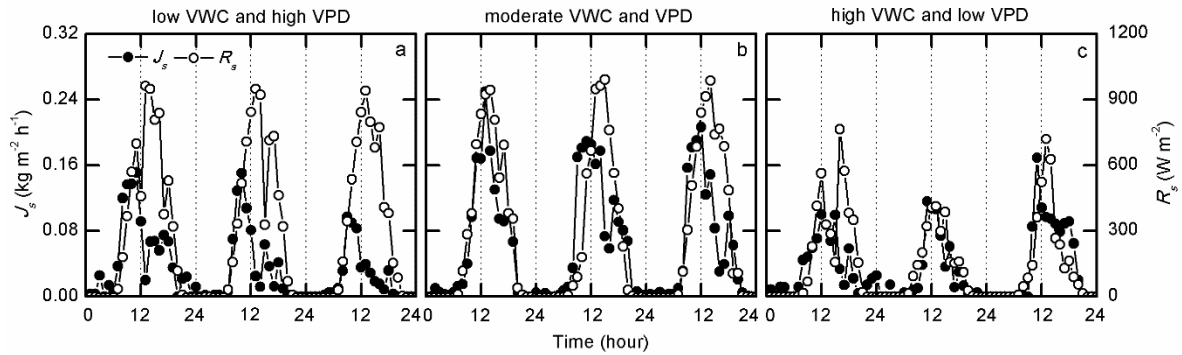
649 **Fig. 7** Seasonal variation in hysteresis loops between sap-flow rate per leaf area (J_s) and
650 shortwave radiation (R_s) using normalized plots for both 2013 and 2014. The y-axis
651 represents the proportion of maximum J_s (dimensionless), and the x-axis represents the
652 proportion of maximum R_s (dimensionless). The curved arrows indicate the clockwise
653 direction of response during the day.

654

655

656

657

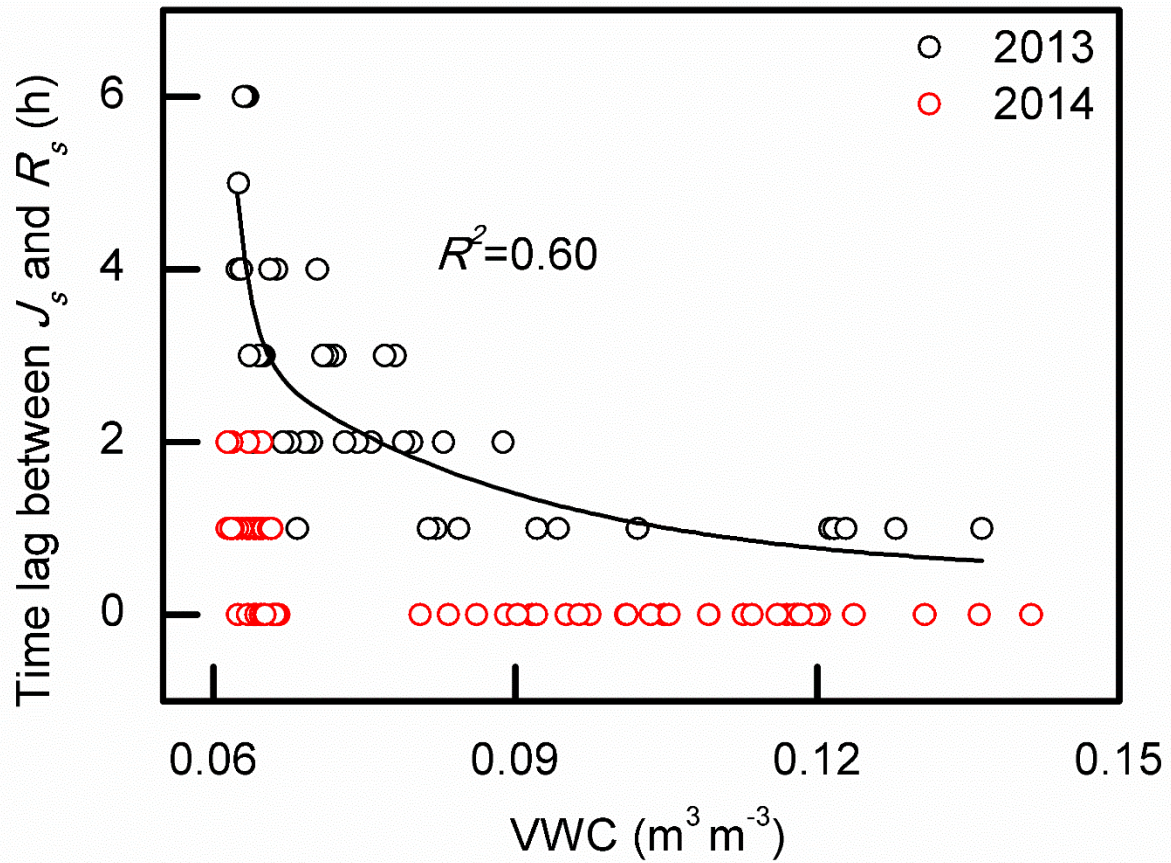


658

659

660 **Fig. 8** Sap-flow rate per leaf area (J_s) and shortwave radiation (R_s) over consecutive three
661 days in 2013, i.e., (a) under low volumetric soil water content (VWC) and high vapor pressure
662 deficit (VPD; DOY 153-155, VWC=0.064 $\text{m}^3 \text{m}^{-3}$, REW=0.025, VPD=2.11 kPa), (b)
663 moderate VWC and VPD (DOY 212-214, VWC=0.092 $\text{m}^3 \text{m}^{-3}$, REW=0.292, VPD=1.72
664 kPa), and (c) high VWC and low VPD (DOY 192-194, VWC=0.152 $\text{m}^3 \text{m}^{-3}$, REW=0.865,
665 VPD= 0.46 kPa). REW is the relative extractable soil water. VWC, REW, and VPD are the
666 mean value of the three days.

667



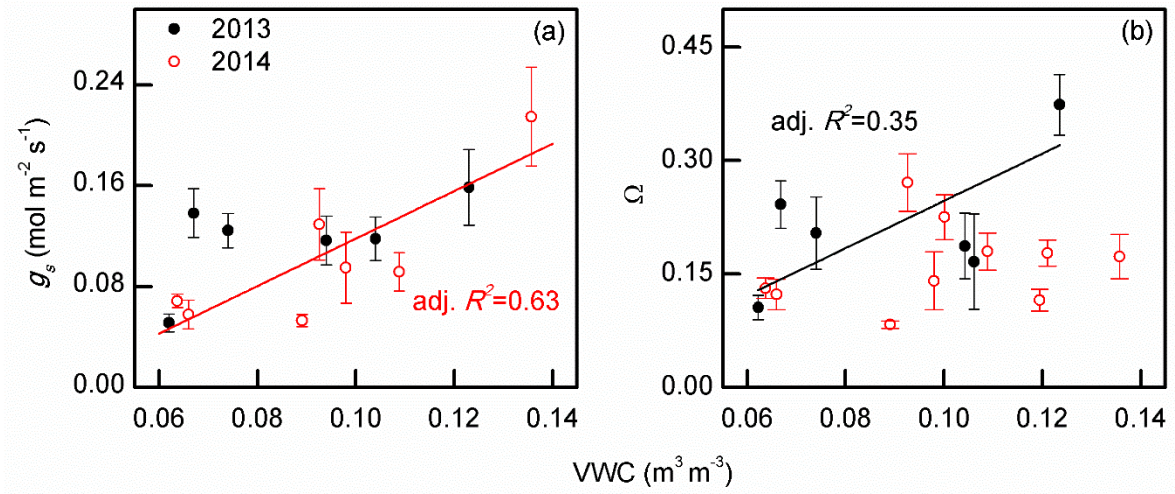
668

669

670 **Fig. 9** Time lag between sap-flow rate per leaf area (J_s) and short wave radiation (R_s) in
 671 relation to volumetric soil water content (VWC). Hourly data in non-rainy days during the
 672 mid-growing season of June 1-August 31 for 2013 and 2014. The lag hours were calculated
 673 by a cross-correlation analysis using a three-day moving window with a one-day time step.
 674 Rainy days were excluded. The solid line is based on exponential regression ($p < 0.05$).

675

676



677

678

679 **Fig. 10** Relationship between volumetric soil water content (VWC) and (a) stomatal
680 conductance (g_s) in *Artemisia ordosica*, and (b) decoupling coefficient (Ω) for 2013 and 2014.

681 Hourly values are given as binned averages based on a VWC-increment of 0.005 m³ m⁻³.

682 Bars indicate standard error. Only regressions with p -values < 0.05 are shown.

683